

## Long-period SU UMa dwarf nova V1006 Cygni: outburst activity and variability at different brightness states in 2015 – 2017

E.P. Pavlenko<sup>1</sup>, S.Yu. Shugarov<sup>2,3</sup>, A.O. Simon<sup>4</sup>, A.A. Sosnovskij<sup>1</sup>,  
K.A. Antonyuk<sup>1</sup>, O.I. Antonyuk<sup>1</sup>, A.V. Shchurova<sup>2</sup>, A.V. Baklanov<sup>1</sup>,  
Ju.V. Babina<sup>1</sup>, A.S. Sklyanov<sup>5</sup>, V.V. Vasylenko<sup>4</sup>, V.G. Godunova<sup>6</sup>,  
I. Sokolov<sup>7</sup> and I.V. Rudakov<sup>8</sup>

<sup>1</sup> *Federal State Budget Scientific Institution “Crimean Astrophysical  
Observatory of RAS”, Nauchny, 298409, Republic of Crimea*

<sup>2</sup> *Astronomical Institute of the Slovak Academy of Sciences  
059 60 Tatranská Lomnica, The Slovak Republic*

<sup>3</sup> *Sternberg Astronomical Institute, Moscow State University, Universitetskij  
pr., 13, Moscow, 119991, Russia*

<sup>4</sup> *Astronomy and Space Physics Department, Taras Shevshenko National  
University of Kyiv, Volodymyrska str. 60, Kyiv, 01601, Ukraine*

<sup>5</sup> *Kazan (Volga region) Federal University, Kazan, 420008, Kremlyovskaya 18,  
Russia*

<sup>6</sup> *ICAMER Observatory of NASU 27 Acad. Zabolotnoho str. 03143, Kyiv,  
Ukraine*

<sup>7</sup> *Institute of Astronomy, Russian Academy of Sciences, Terskol Branch,  
Settlement Terskol, Kabardino-Balkarian Republic, 361605, Russian  
Federation*

<sup>8</sup> *Observatory of the National Scientific and Practical, Educational and  
Wellness Center “Bobek”, Askarov str. 47, Almaty, 050027, Republic of  
Kazakhstan*

Received: March 26, 2018; Accepted: May 9, 2018

**Abstract.** CCD photometric observations of the dwarf nova V1006 Cyg were carried out in 2015 – 2017 with 11 telescopes located at 7 observatories. They covered the 2015 superoutburst with rebrightening, five normal outbursts of  $\sim 4$ -day duration and one wide outburst that lasted at least seven days. The interval between normal outbursts was 16 and 22 days, and between superoutbursts is expected to be longer than 124 days. The positive superhumps with the mean period of  $0^d.10544(10)$  and  $0^d.10406(17)$  were detected during the 2015 superoutburst and during the short-term quiescence between rebrightening and the start of the first normal outburst, respectively. During a wide 2017 outburst the orbital period  $0^d.09832(15)$  was found. The amplitude of this signal was  $\sim 2.5$  times larger at the outburst decline than at its end. During the quiescence stage between the first and the second normal outbursts in 2015 we possibly detected the negative superhumps with the period of  $0^d.09714(7)$ .

In all other cases of quiescence we found only the quasi-periodic brightness variations on a time scale of 20–30 minutes with a different degree of coherence and a variable amplitude reaching 0.5 mag in extremal cases.

**Key words:** dwarf novae – superhumps – photometry – rapid variability

## 1. Introduction

Dwarf novae are a subclass of cataclysmic variables. They consist of a pair of dwarfs. The red (or brown) dwarf fills in its Roche Lobe and loses material onto the white dwarf, creating an accretion disk around it (Warner 1995). The matter in the disk accumulates until reaching some critical conditions that are necessary for the transition of the disk from the cool and neutral one to the hot and ionized one. This thermal disk instability (Osaki 1996; Hoshi 1979; Meyer and Meyer-Hofmeister 1981) leads to the dwarf nova outburst. SU UMa-type dwarf novae are a special subclass of the dwarf novae possessing two types of outbursts – normal outbursts and superoutbursts. Several normal outbursts that have a typical duration of 2–5 days and an outburst amplitude of 2–3 mag are placed between superoutbursts. The last ones have a higher amplitude and longer duration (Warner 1995). The time between neighboring superoutbursts (supercycle) is a more-or-less stable value and could be a characteristic of the dwarf nova. Thus stars with a supercycle  $< 100^d$  are called “active” dwarf novae, these with the shortest (19–48 days) supercycles are ER UMa-type dwarf novae (Kato *et al.* 2013). WZ-type dwarf novae have the longest supercycles lasting years – decades (Kato 2015). There could be several cycles (time between normal outbursts) during the supercycle. Both types of outbursts are considered to be a result of the combination of thermal and tidal instabilities (Osaki 1989; Osaki 1996).

Only during the outbursts the periodic brightness variations (so-called “positive superhumps”) with a period of a few percent longer than the orbital one are observed. According to a modern point of view, these superhumps originate from a precessing eccentric disk, and eccentricity that is believed to be caused by the 3:1 resonance in the disk (Whitehurst 1988; Hirose and Osaki 1990; Lubow 1991; Wood *et al.* 2011). The requirement for the noted resonance is the mass ratio of the components  $m_2/m_1 < 0.3$  that is implemented for SU UMa stars with orbital periods between 76 min and 3.18 hours (Knigge 2006). These periods include a known “period gap” between 2 and 3 hours for the cataclysmic variables distribution. However, as it was shown on the basis of a large number of examples (Pavlenko *et al.* 2014; Kato *et al.* 2017a), SU UMa stars in the period gap display rather extension of monotonic decrease of the stars number toward the long-periodic border of the gap instead of an abrupt shortage of them.

In any state of the outburst activity there could be variations that are a few percent less than the orbital one – so-called “negative superhumps” (Udalski 1988; Harvey *et al.* 1995; Ringwald *et al.* 2012). The origin of negative super-

humps is usually considered as a result of retrograde precession of a tilted accretion disk (Wood, Burke 2007). The number of known negative superhumpers is much smaller than that of known positive superhumpers among SU UMa stars and currently comprises about 15 binaries (Pavlenko, under preparation).

V1006 Cyg was discovered as a dwarf nova by Hoffmeister (1963a, 1963b) with a photographic range of 16–18 mag. Gessner (1966) and Bruch et al. (1987) found it in an outburst later on. Bruch and Schimpke (1992) also identified this object as a dwarf nova from its spectrum. Sheets et al. (2007) used radial velocities to find the orbital period of  $0^d.09903(9)$ . The second time V1006 Cyg was found in rather wide outbursts lasting more than six days in 2007 and more than five days in 2009 (Pavlenko et al. 2014), but no superhumps were observed. Instead the orbital period was detected in both outbursts by Pavlenko et al. (2014).

Kato et al. (2016) informed that the start of the first genuine superoutburst of V1006 Cyg was detected on July, 12 2015 by Shappee et al. by the All-Sky Automated Survey for Supernovae (ASAS-SN). The 2015 superoutburst was studied in detail by the VSNET campaign (Kato et al. 2016). The  $0^d.10541$  superhump period was found that finally established this object to be an SU UMa-type dwarf nova in the period gap, i.e, a long-periodic SU UMa dwarf nova. Recently, Kato et al. (2009) showed that the evolution of superhumps of SU UMa stars has three stages. These stages were also found in the period of superhump variations of V1006 Cyg (Kato et al. 2016). The authors estimated mass ratio for this binary as 0.26-0.33 solar masses. However, the cycle, supercycle of V1006 Cyg and its behavior in quiescence was unknown. This motivated us to undertake the next multi-site campaign on a long-term study of this dwarf nova immediately at the end of the VSNET campaign.

## 2. Observations and data reduction

Photometric investigations of V1006 Cyg have been carried out with 11 telescopes located at 7 observatories in photometric system close to the Johnson - Cousins  $UBVR_CI_C$  system or in the integral light (symbol "C"), see Table 1: Journal of observations. In this paper we analyse only  $BVR_C$  data. The standard data reduction included a flat-fielding, bias and dark signal removal. We used the MAXIM DL and V. Goranskij (<http://www.vgoranskij.net/software/>) WinFit packages to measure the brightness of variable, comparison and check stars. The data were referred to AAVSO comparison star No 140. Its brightness was measured relatively to the known magnitudes in the vicinity of CH Cyg (Henden and Munari, 2006). For this star we obtained  $B = 14^m.89, V = 13^m.99, R_C = 13^m.47, I_C = 13^m.03$ . The corresponding AAVSO data are  $B = 14^m.96, V = 13^m.96, R_C = 13^m.45, I_C = 12^m.97$ . For the analysis we used our data. We combined the data from different locations by adding the corresponding corrections which we calculated for common nights of observations for different telescopes. The intrinsic accuracy was measured as a standard devia-

tion for the number of check stars in regard to the comparison one. It depended on the telescope, weather condition, exposure time and the brightness of object. At the maximum it was  $0^m.005 - 0^m.05$  and at minima  $0^m.03 - 0^m.1$ .

**Table 1.** Journal of observations.  $JD = JD^* + 2\,450\,000$ .

Date	JD*start-end	N	Tel.	Obs.	CCD	Band	Stage
<b>2015</b>							
17.07	7221.279-.380	87	2.6m	CrAO	APOGEE E47	Rc	S
18.07	7222.262-.564	97	50cm	SAI	APOGEE A1.U16	CUBVRcIc	S
19.07	7223.291-.564	92	50cm	SAI	APOGEE A1.U16	CUBVRcIc	S
20.07	7224.225-.264	11	50cm	SAI	APOGEE A1.U16	CUBVRcIc	S
20.07	7224.271-.546	230	38cm	CrAO	APOGEE E47	C	S
21.07	7225.225-.299	28	50cm	SAI	APOGEE A1.U16	CUBVRcIc	S
21.07	7225.264-.547	191	38cm	CrAO	APOGEE E47	C	S
21.07	7226.224-.290	22	50cm	SAI	APOGEE A1.U16	CUBVRcIc	S
22.07	7226.547-.460	72	38cm	CrAO	APOGEE E47	C	S
23.07	7227.280-.552	240	38cm	CrAO	APOGEE E47	C	S
24.07	7228.279-.558	186	38cm	CrAO	APOGEE E47	C	S
25.07	7229.269-.563	183	38cm	CrAO	APOGEE E47	C	S
26.07	7230.275-.562	126	38cm	CrAO	APOGEE E47	C	S
27.07	7231.348-.564	200	38cm	CrAO	APOGEE E47	C	R
28.07	7232.278-.567	197	38cm	CrAO	APOGEE E47	C	R
29.07	7233.256-.564	195	38cm	CrAO	APOGEE E47	C	R
30.07	7234.262-.555	198	38cm	CrAO	APOGEE E47	C	Q
31.07	7235.283-.558	182	38cm	CrAO	APOGEE E47	C	Q
31.07	7235.367-.548	124	60cm	SL	FLI ML3041	CBVRcIc	Q
01.08	7236.254-.525	124	38cm	CrAO	APOGEE E47	C	Q
01.08	7236.316-.542	178	60cm	SL	FLI ML3041	C	Q
02.08	7237.377-.560	71	38cm	CrAO	APOGEE E47	C	Q
02.08	7237.465-.339	143	60cm	SL	FLI ML3041	C	Q
03.08	7238.288-.545	102	38cm	CrAO	APOGEE E47	C	O1
03.08	7238.303-.323	17	18cm	SL	SBIG ST-10XME	C	O1
04.08	7239.247-.571	177	38cm	CrAO	APOGEE E47	C	O1
04.08	7239.298-.550	79	18cm	SL	SBIG ST-10XME	C	O1
04.08	7239.387-.516	50	28cm	KFU	QSI 583wsg	C	O1
05.08	7240.269-.566	401	38cm	CrAO	APOGEE E47	C	Q
06.08	7241.337-.499	49	28cm	KFU	QSI 583wsg	C	Q
07.08	7242.277-.504	60	28cm	KFU	QSI 583wsg	C	Q
07.08	7242.252-.558	200	38cm	CrAO	APOGEE E47	C	Q
08.08	7243.289-.211	60	28cm	KFU	QSI 583wsg	C	Q
08.08	7243.254-.358	235	2.6m	CrAO	APOGEE E47	C	Q
09.08	7244.377-.398	47	2.6m	CrAO	APOGEE E47	C	Q
09.08	7244.314-.592	153	60cm	SL	FLI ML3041	C	Q
10.08	7245.211-.506	99	28cm	KFU	QSI 583wsg	C	Q
10.08	7245.409-.593	102	60cm	SL	FLI ML3041	C	Q
11.08	7246.218-.449	80	28cm	KFU	QSI 583wsg	C	Q

**Table 1.** Continued.

Date	JD*start-end	N	Tel.	Obs.	CCD	Band	Stage
11.08	7246.548-.588	23	60cm	SL	FLI ML3041	C	Q
12.08	7247.238-.351	17	28cm	KFU	QSI 583wsg	C	Q
13.08	7248.204-.501	91	28cm	KFU	QSI 583wsg	C	Q
14.08	7249.279-.307	17	38cm	CrAO	APOGEE E47	C	Q
15.08	7250.340-.375	24	38cm	CrAO	APOGEE E47	C	Q
16.08	7251.302-.333	22	38cm	CrAO	APOGEE E47	C	Q
17.08	7252.317-.356	26	38cm	CrAO	APOGEE E47	C	O2
17.08	7252.370-.378	5	125cm	CrAO	ProLine 23042	Rc	O2
18.08	7253.360-.362	5	125cm	CrAO	ProLine 23042	VRcIc	O2
18.08	7253.302-.470	113	38cm	CrAO	APOGEE E47	C	O2
19.08	7254.349-.403	22	125cm	CrAO	ProLine 23042	VRcIc	O2
20.08	7255.318-.375	25	125cm	CrAO	ProLine 23042	VRcIc	O2
21.08	7256.334-.343	5	125cm	CrAO	ProLine 23042	VRcIc	O2
24.08	7259.260-.271	5	125cm	CrAO	ProLine 23042	VRcIc	Q
25.08	7260.274-.295	9	125cm	CrAO	ProLine 23042	VRcIc	Q
26.08	7261.316-.321	3	125cm	CrAO	ProLine 23042	VRcIc	Q
27.08	7262.302-.306	3	125cm	CrAO	ProLine 23042	Rc	Q
28.08	7263.343-.347	3	125cm	CrAO	ProLine 23042	VRcIc	Q
29.08	7264.266-.270	3	125cm	CrAO	ProLine 23042	VRcIc	Q
31.08	7266.297	1	70cm	Lisnyky	FLI PL4710	UBVRcIc	Q
01.09	7267.334	1	70cm	Lisnyky	FLI PL4710	UBVRcIc	Q
01.09	7267.258-.354	45	125cm	CrAO	ProLine 23042	Rc	Q
02.09	7268.259-.268	5	125cm	CrAO	ProLine 23042	Rc	Q
02.09	7268.284	1	70cm	Lisnyky	FLI PL4710	UBVRcIc	Q
03.09	7269.257-.349	43	125cm	CrAO	ProLine 23042	Rc	Q
04.09	7270.393-.567	723	2.6m	CrAO	APOGEE E47	C	Q
08.09	7274.248-.256	5	125cm	CrAO	ProLine 23042	Rc	Q
09.09	7275.244-.248	3	125cm	CrAO	ProLine 23042	Rc	O3
09.09	7275.453-.571	207	2.6m	CrAO	APOGEE E47	C	O3
10.09	7276.247-.259	6	125cm	CrAO	ProLine 23042	Rc	O3
11.09	7277.257-.475	97	125cm	CrAO	ProLine 23042	VRcIc	O3
15.09	7280.248-.257	5	125cm	CrAO	ProLine 23042	Rc	Q
15.09	7281.228-.232	3	125cm	CrAO	ProLine 23042	Rc	Q
15.09	7281.277	1	70cm	Lisnyky	FLI PL4710	UBVRcIc	Q
16.09	7282.368-.473	50	125cm	CrAO	ProLine 23042	Rc	Q
16.09	7282.297	1	70cm	Lisnyky	FLI PL4710	UBVRcIc	Q
17.09	7283.400-.445	22	125cm	CrAO	ProLine 23042	Rc	Q
17.09	7283.260	1	70cm	Lisnyky	FLI PL4710	Rc	Q
18.09	7284.230-.476	110	125cm	CrAO	ProLine 23042	Rc	Q
18.09	7284.250	1	70cm	Lisnyky	FLI PL4710	UBVRcIc	Q
19.09	7285.334	1	70cm	Lisnyky	FLI PL4710	Rc	Q
20.09	7286.334	1	70cm	Lisnyky	FLI PL4710	UBVRcIc	Q
22.09	7288.242	1	70cm	Lisnyky	FLI PL4710	UBVRcIc	Q
25.09	7291.374	1	70cm	Lisnyky	FLI PL4710	UBVRcIc	Q
05.10	7301.134	1	60cm	Almaty	SXVR-35H	C	Q

**Table 1.** Continued.

Date	JD*start-end	N	Tel.	Obs.	CCD	Band	Stage
06.10	7302.198	1	60cm	Almaty	SXVR-35H	C	Q
07.10	7303.252	1	60cm	Almaty	SXVR-35H	C	Q
08.10	7304.240	1	60cm	Almaty	SXVR-35H	C	Q
15.10	7310.306	1	70cm	Lisnyky	FLI PL4710	UBVRcIc	Q
16.10	7311.189-.340	66	38cm	CrAO	APOGEE E47	C	Q
20.10	7315.206-.28	97	38cm	CrAO	APOGEE E47	C	O5
30.10	7325.2	1	38cm	CrAO	APOGEE E47	C	Q
31.10	7326.277	1	70cm	Lisnyky	FLI PL4710	Rc	Q
01.11	7327.244	1	70cm	Lisnyky	FLI PL4710	Rc	Q
05.11	7332.149-.274	172	125cm	SAI	VersAray1300	C	Q
11.11	7338.258	1	70cm	Lisnyky	FLI PL4710	Rc	Q
24.12	7381.215	1	70cm	Lisnyky	FLI PL4710	Rc	Q
<b>2016</b>							
2.04	7481.449-.600	180	2.6m	CrAO	APOGEE E47	BVRc	Q
5.05	7514.430-.505	216	2.6m	CrAO	APOGEE E47	C	Q
20.08	7621.359-.580	47	70cm	Lisnyky	FLI PL4710	UBVRcIc	O6
21.08	7622.289-.578	115	70cm	Lisnyky	FLI PL4710	UBVRcIc	O6
<b>2017</b>							
16.10	8043.257-.406	201	70cm	Lisnyky	FLI PL4710	UBVRcIc	O8W
16.10	8043.178-.451	376	38cm	CrAO	APOGEE E47	C	W
17.10	8044.217-.393	483	38cm	CrAO	APOGEE E47	C	W
18.10	8045.206-.364	214	38cm	CrAO	APOGEE E47	C	W
19.10	8046.208-.359	103	38cm	CrAO	APOGEE E47	C	W
25.11	8083.285-.380	124	2m	Terskol	FLI PL4301	B	Q
27.11	8085.228-.373	191	2m	Terskol	FLI PL4301	B	Q

**Description of columns:**

Date: calendar data.

JD\* start-end: beginning and end of the observational run.

N - number of observations.

Tel.: size of the telescope's objective.

Obs. – Observatory: CrAO - Crimean Astrophysical Observatory, Republic of Crimea; SL - Stará Lesná Observatory of the Astronomical institute of the Slovak Academy of Sciences, Slovakia; SAI - Southern Station of the Sternberg Astronomical Institute, Crimea; Lisnyky - Taras Shevchenko National University of Kyiv, Ukraine; Almaty - Observatory of the NSPEWC Bobek, Republic of Kazakhstan; Terskol - Terskol observatory, Russian Academy of Sciences, Terskol Branch, Settlement Terskol, Kabardino-Balkarian Republic; KFU - North-Caucasus Astronomical Station of Kasan Federal University.

CCD: CCD camera type, abbreviation "APOGEE Al.U16" is APOGEE Alta U16M.

Band: passband  $UBVR_cI_c$ , C-integral light.

Stage: Designations of activity types: S - superoutburst, R - rebrightening, W - wide outburst without superhumps, O - normal outburst, Q - quiescence.

In the case of a low signal-to-noise ratio the data have been stacked to reach the acceptable accuracy. We used the Stellingwerf method for the time-series analysis with Pelt package ISDA (Pelt 1980).

### 3. Analysis of the 2015-17 light curves

#### 3.1. Long-term light curve, cycles and supercycle

We observed V1006 Cyg since its 2015 superoutburst from July 17, 2015 till November 27, 2017 during 81 days (106 runs of observations). The long-term light curve based on the most dense part of the 2015 observations is shown in Fig. 1. The amplitude of the superoutburst in the  $R_C$ -band was  $\sim 3^m.5$ . It lasted about 18-19 days, including rebrightening and taking into account that the start of the superoutburst was around JD 2457216 according to the VSNET announcement. Note that this duration was the same as those of another dwarf novae in the period gap NY Ser (Pavlenko et al. 2014, Sklyanov et al. 2018) and MN Dra (Sklyanov et al. in preparation). The amplitude of normal outbursts was a few tenths of magnitude less and varied, which is caused by the large variations of the quiescent brightness.

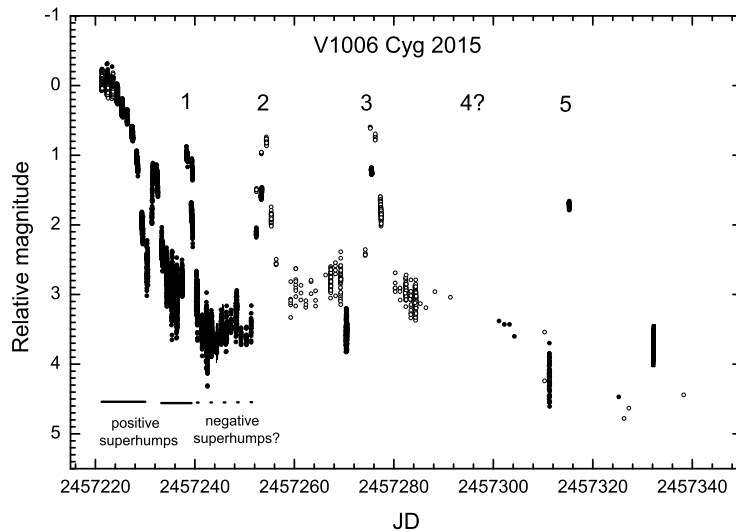


**Figure 1.** The V1006 Cyg light curve in 2015.  $R_C$  data and unfiltered data are shown by open and filled circles, respectively. The data are expressed relatively the comparison star No 140. The sequence of the normal outbursts (including a possible outburst No 4) is numbered. For JD 2457221 – 2457246 the types of periodicity are indicated.

The first normal outburst occurred 6 days after the superoutburst rebrightening. The cycle between the first and the second normal outburst lasted 16 days, while the cycle between the second and the third one 22 days. The next cycle was undefined because of a lack of observations between JD 2457292 – 2457301. Potentially a normal outburst could occur in this interval, that is too short for the superoutburst. Taking into account that the last 2015 normal outburst was detected in  $\sim 124$  days after the start of superoutburst and there was no possibility for the next superoutburst to occur up to JD 2457339, we could conclude that the supercycle should be longer than 124 days. It means that V1006 Cyg is not an active dwarf nova.

### 3.2. Superoutburst

We have studied the brightness variability of V1006 Cyg during the first 25 nights since the start of the 2015 superoutburst that covered main superoutburst, rebrightening and the first normal outburst. The results are presented in Fig. 2.

Positive superhumps, with mean period  $P_1 = 0^d.10544(10)$ , were detected during the superoutburst. During the short-term quiescence between the rebrightening and the start of the first normal outburst the mean period of positive superhumps was  $P_2 = 0^d.10406(17)$ . These periods are in agreement with periods found by Kato et al. (2016) from the detailed study of the positive superhumps evolution during JD 2457219 – 2457240. A periodogram in quiescence after the first normal outburst points to the most significant peaks  $P_4 = 0^d.107594(85)$  and  $P_5 = 0^d.097142(74)$  that are not independent but are the day-aliased. There is also a peak at a period  $P_3$  coinciding with the period of positive superhumps  $P_2$  but of lower significance, and no indication of the orbital period. From two periods  $P_4$  and  $P_5$  we prefer the latter because it is closer to a potentially possible period of negative superhumps.

Using the values of the orbital period  $P_{orb} = 0^d.09903$ , the positive superhump period  $P_2 = 0^d.104062$  and the suggestive negative superhump period  $P_5 = 0^d.09714$ , one could calculate a positive superhump period excess  $\epsilon^+ = (P_{+sh} - P_{orb})/P_{orb}$  and a negative superhump period deficit  $\epsilon^- = (P_{-sh} - P_{orb})/P_{orb}$ , where  $P_{+sh}$  and  $P_{-sh}$  are the periods of positive and negative superhumps, respectively. We obtained  $\epsilon^+ = 0.051$ ,  $\epsilon^- = -0.019$  and  $\phi = \epsilon^-/\epsilon^+ = -0.037$ .

Our data are in good agreement with an empirical relation between  $\epsilon^+$ ,  $\epsilon^-$  and the orbital period (Hellier, 2001). Moreover, we found that the ratio  $\epsilon^-/\epsilon^+ = -0.037$  corresponds to the mass ratio  $q \sim 0.30 - 0.32$  according to the Wood's et al. (2009) model, that coincides with an independent estimate of Kato et al (2016),  $q \sim 0.26 - 0.33$ . So we can conclude that our identification of the period  $0^d.09714$  as the period of negative superhumps is correct.

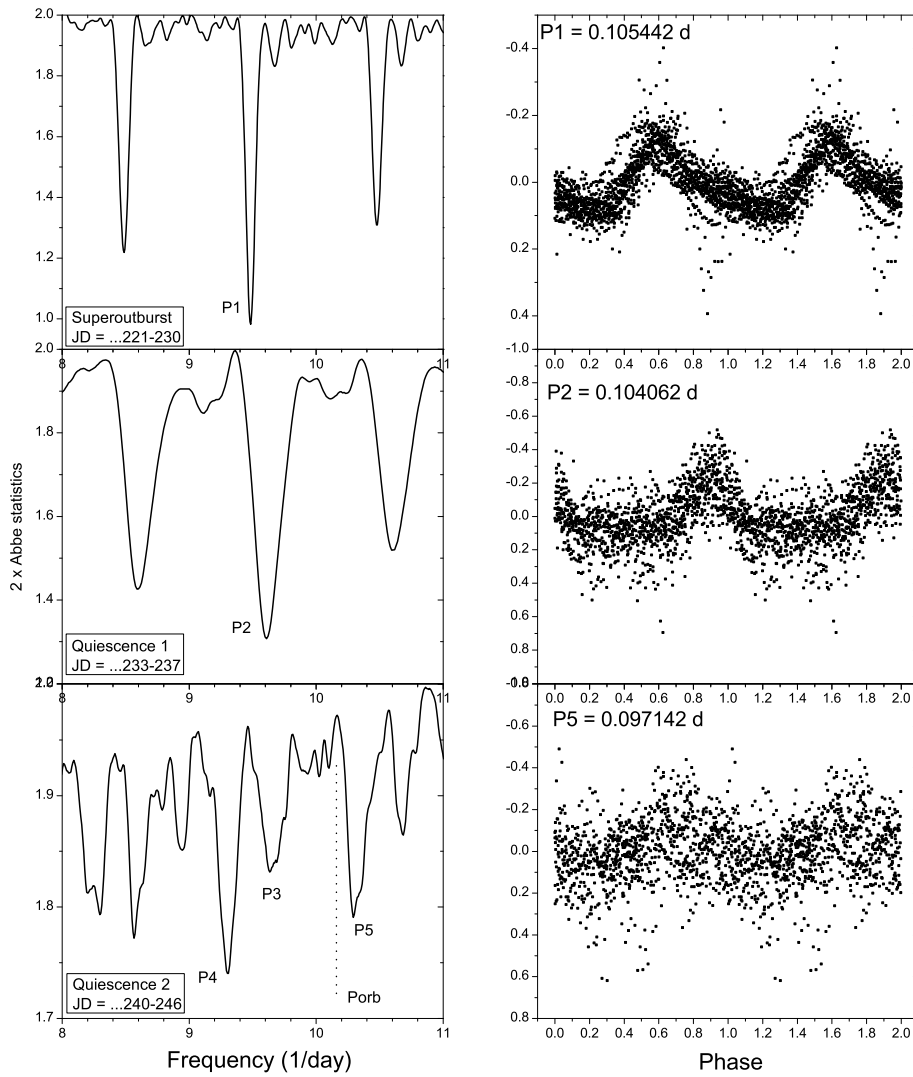


**Figure 2.** Left (from top to bottom): the periodograms for the superoutburst, short-term quiescence between rebrightening and the first normal outburst and quiescence between the first and the second normal outbursts. For every data set the time interval is indicated. The designations of peaks are given in the text. The position of the orbital period is marked by the dotted line. The phase diagrams of corresponded data folded with the most significant periods are presented on the right.

### 3.3. Normal outbursts

We gathered all our measured colour-indices  $V - R_C$  for different stages of activity of V1006 Cyg and presented them in the color-magnitude diagram (Fig.3). All the data are attributed to the outburst decline. Unfortunately no color measurement were done at the rising part of the outbursts. Therefore, we cannot decide whether the tracks corresponding to ascending and descending branches of outbursts are the same, or they perform a loop as it was found by Smak (1978).

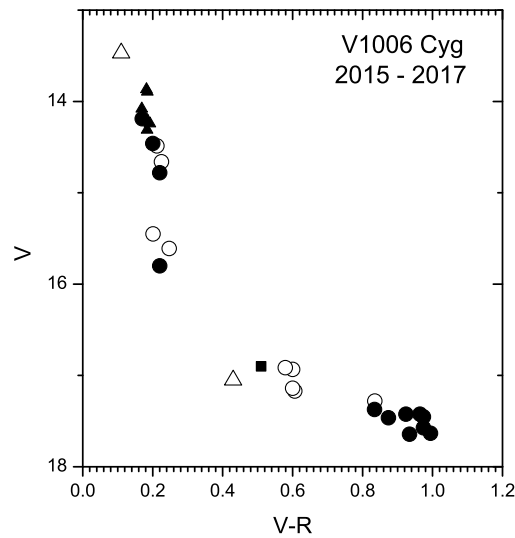


**Figure 3.** The color-magnitude diagram for different stages of the 2015 super-outburst, normal outbursts No 1, 2, 3 (2015) and the wide outburst (2017). The filled triangles, open circles, filled circles, filled triangles, filled square and open squares denote the mean per night data obtained with 2.6-m, 1.25-m, 70-cm, 60-cm and 50-cm telescopes respectively.

The peculiarity of this color-magnitude behavior resembles those of other dwarf novae (Pavlenko et al. 2008): the small reddening during the  $\sim 2^m$  brightness decline after the outburst maximum and much faster reddening during the slower approach to the quiescence and in quiescence itself. Such behavior is probably caused by a different contributions of the sources of radiation to the total light during the outburst: a decrease of accretion disk role and increase of the secondary component role with outburst decline.

### 3.4. 2017 wide outburst

In 2017 we observed a wide outburst with the amplitude of about 3.5 mag. The AAVSO and our data suggest its duration at least seven days (Fig. 4). During

the wide outburst decline we detected the periodic brightness variations in four subsequent nights. To search for the period and to compare an amplitude of periodicity we converted detrended data of four nights into relative intensities  $I_{rel}$  according to the formula  $I_{rel} = 10^6 \cdot 10^{-0.4 \cdot m}$ , where  $m$  is expressed in  $R_C$ -magnitudes.

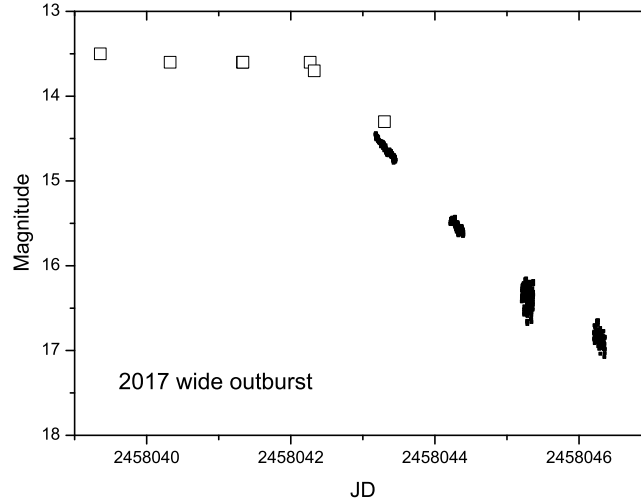


**Figure 4.** The 2017 wide outburst. Open and solid squares denote the AAVSO ([www.aavso.org](http://www.aavso.org)) and our data respectively.

The periodogram is presented in Fig. 5 (the upper panel). The most significant peak among day-aliased peaks points to a period of  $0^d.09832(15)$ , which coincides with the known orbital period (Pavlenko et al. 2014). Note that there were two known events of wide outbursts in 2007 and 2009 without superoutbursts, but with the orbital periodicity. The mean phase light curve is given in the middle panel of Fig. 5. In the lower panel we show the smoothed phase light curves for the wide outburst decline. One could see that the amplitudes of the data for the first three nights are near equal, while the amplitude of the data of last night data is close to quiescence is  $\sim 2.5$  times lower.

We also detected the outburst in August 2016 during the brightness rise and the maximum in two subsequent nights. However, a lack of further data does not allow us to specify if this was a wide or normal outburst. Since our observation at the maximum lasted about 6.5 hours, we were able to examine brightness variations around the orbital period, too. We constructed the periodogram for the  $V$  and  $R_C$  data combined together (their amplitudes are almost equal) and plotted it in the upper frame of Fig. 5. It can be seen that this periodogram also points to the periodicity around the orbital period.

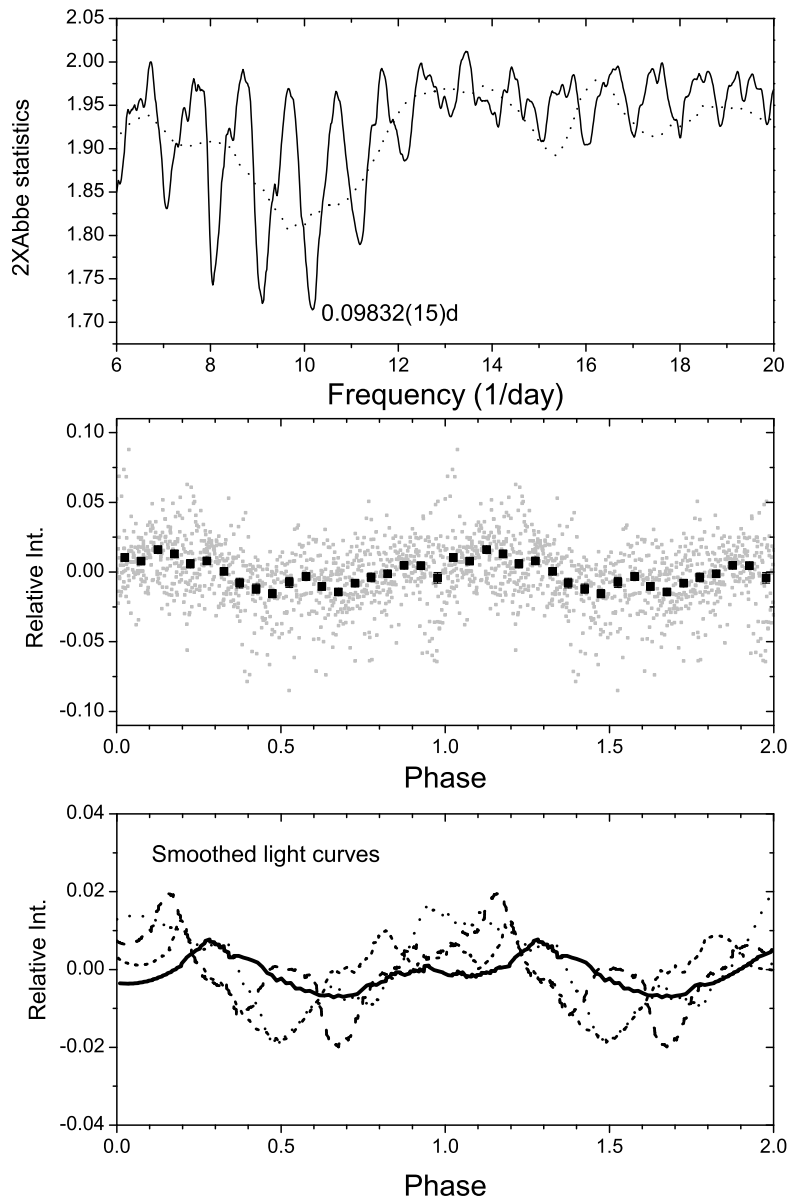


**Figure 5.** Top: the periodogram for the data of the 2017 wide outburst decline (the solid line). The periodogram for the data of a single night of the 2016 outburst is shown by the dotted line. Middle: the mean phase light curve for the data of the wide outburst. Bottom: the original smoothed phase light curves of the wide outburst on 3 subsequent nights (dash and dotted lines). The phase light curve for the last night of the wide outburst is expressed by the solid thick line.

### 3.5. Quiescence

Observations of V1006 Cyg in quiescence (out of the outbursts) were carried out in 2015, 2016 and 2017 (see Table 1). Contrary to expectations, we did not detect a prominent orbital modulation in this state. This may indicate the low inclination of the binary orbit. Instead, the examples of the long runs of observations demonstrate one and the same feature of the nightly light curves - more or less strong quasi-periodic oscillations of a variable frequency and amplitude. The amplitude could reach on some occasions  $\sim 0^m.5$ . The examples of nightly light curves and corresponding periodograms are shown in Fig. 6. The  $BVR_C$  observations for JD 2457481 showed that the amplitude of oscillations is practically the same in the  $V$ - and  $R_C$ - passband while in  $B$ -passband it is slightly higher. The significance of the quasi-period depends on the amplitude of QPO and a coherence time.

For every night we selected the more significant periods (for definiteness the periods with significance  $< 1.6$ ). The results are given in Table 2 and in the histogram (Fig. 7). The maximal number of quasi-periods is observed in the interval 20-30 minutes that is 5-7 times shorter than the orbital period. The quasi-periods between 50-60 min probably are doubles of those between 20-30 min. Note that the potential orbital modulation is probably hidden by QPOs.

It is possible to find similar high-amplitude QPOs in CVs that have no relation to their orbital periods. The behavior and nature of QPOs at various states of cataclysmic variables activity may be different (see e.g.: Kato et al. 2017b; Shugarov et al. 2016; Pavlenko and Shugarov 1999; Scaringi et al. 2017; Pavlenko 1996; Zemko et al. 2014). A detailed study of QPOs in CVs in quiescence during quiescence is limited by the faintness of these objects.

Our results are in good agreement with the model of compactness in an accretion disk described by Fridman and Bisikalo (2008). According to their model, there could appear a coagulate in an accretion disk after the binary underwent a decrease of its accretion rate. This coagulate moves with a period of  $\sim 0.15P_{orb} - 0.18P_{orb}$  and could be understood as the one-armed spiral density wave (Fridman et al. 2003; Fridman and Khoruzhii 2003).

**Table 2.** The most significant quasi-periods for selected nights of 2015, 2016 and 2017.

JD	QPO (min)
2457286	53; 96
2457332	30; 115
2457481	18; 26; 36; 51
2457514	18; 23; 33
2458083	29; 63; 90; 120

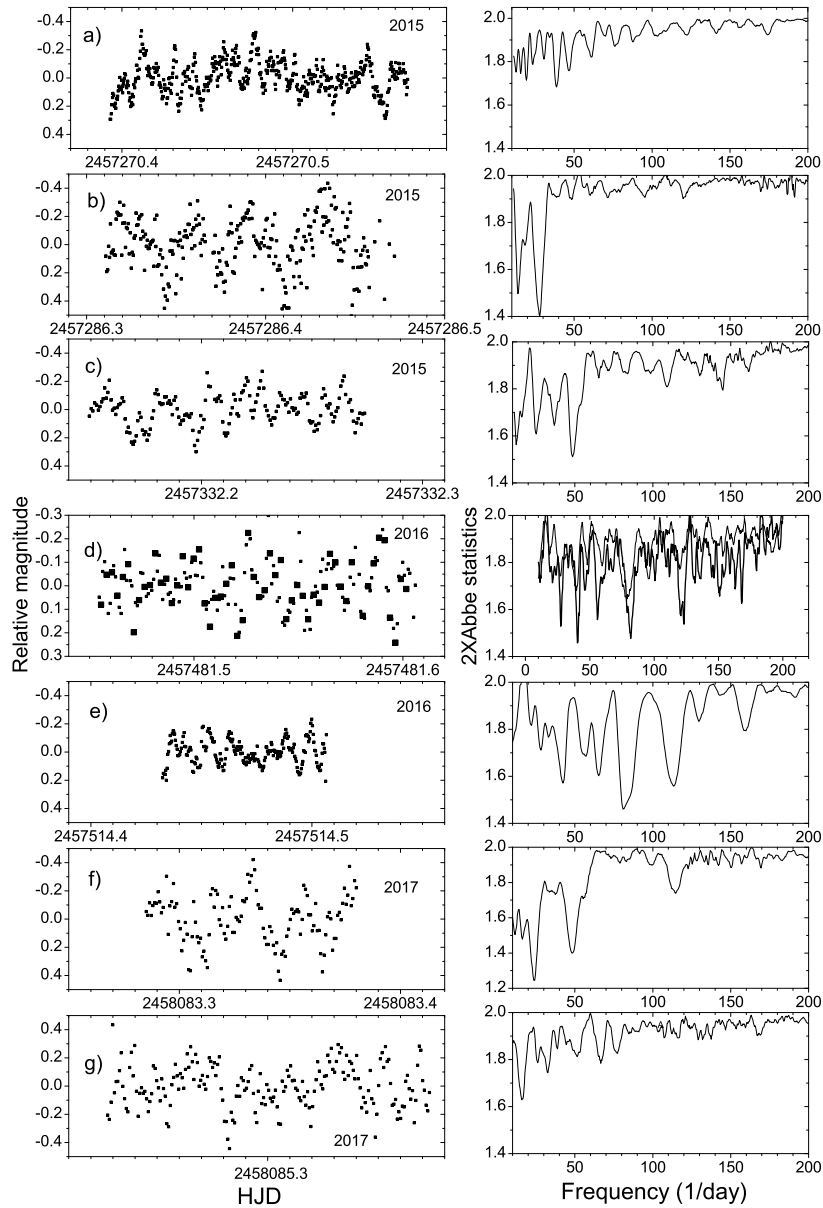


**Figure 6.** Left panels: the examples of nightly light curves of V1006 Cyg during quiescent states in 2015, 2016 and 2017 normalized to the mean brightness level. The light curve at JD 2457481 contains both  $VR_C$  and  $B$  data plotted by dots and bold squares, respectively. Right panels: corresponding periodograms. There are two periodograms for the JD 2457481 on the same graph: the periodograms for  $V R_C$  and  $B$  data are expressed by the thin and bold lines, respectively.

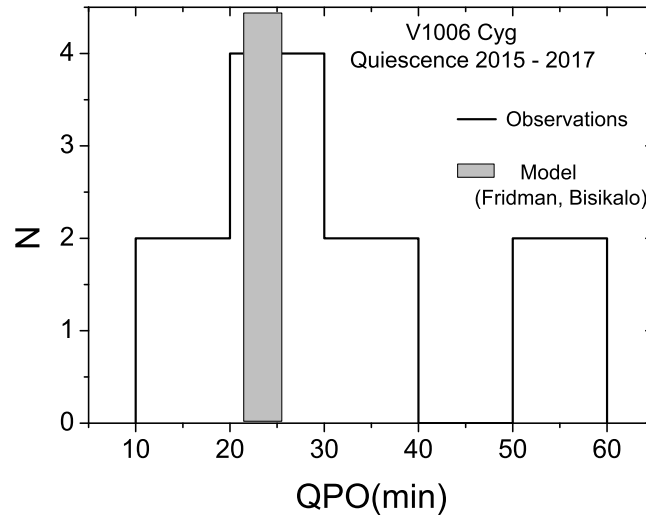


**Figure 7.** The histogram of the formally most significant QPOs observed in quiescences. The gray region corresponds to a range of predicted QPOs according to the Fridman and Bisikalo (2008) model.

#### 4. Conclusion

The detailed study of the SU UMa-type nova-in the gap, V1006 Cyg, allowed us to find the peculiarities of its superoutburst, normal and wide outbursts, and quiescence. We define its activity state as a supercycle that is longer than 124 d and variable cycles that are 16 d and 22 d for the 2015 year. In 2017 we observed a wide outburst similar to those observed in 2007 and 2009 (Pavlenko et al. 2014) that was accompanied, as in the two previous cases, by the orbital brightness variations without superhumps. The orbital signal at the start of the wide outburst decline was 2.5 times higher than those at the end. If the orbital modulation is caused by the hot spot visibility over the orbital period, this could mean a slightly enhanced mass transfer rate. The absence of superoutbursts means a hard achievement of the tidal resonance in every wide outburst for a binary with the critical mass ratio of 0.26–0.33, which is close to the stability limit of the tidal instability (Kato et al. 2016). We found positive superhumps during the 2015 superoutburst that lasted up to the first and probably the second normal outburst. The strongest signal in quiescence between the first two normal outbursts could be a negative superhump. The ratio of the negative superhump period deficit to the positive superhump period excess corresponds to the mass ratio  $q = 0.30 - 0.32$  according to the Wood et al. (2009) model and coincides with  $q \sim 0.26 - 0.32$  found by Kato et al. (2016). The orbital signal in quiescence may be masked by the high-amplitude QPOs caused by a probably low inclination of the orbit. The values of the V1006 Cyg quiescent QPOs are in good agreement with Fridman and Bisikalo (2008) prediction of heterogeneities

in the accretion disk caused by the mass accretion rate decrease.

**Acknowledgements.** The authors thank an anonymous referee for valuable comments and suggestions. This work was partially funded by RFBR according to the research project 18-32-00371, by the subsidy allocated to Kazan Federal University for the state assignment in the sphere of scientific activities (3.9780.2017/8.9); the Russian Government Program of Competitive Growth of Kazan Federal University and was performed with the use of observational data obtained at the North-Caucasus Astronomical Station of KFU; S. Shugarov thanks for partial support the grants VEGA 2/0008/17 and APVV 15-0458. S. Simon is grateful to V.P. Lapchuk for technical help in observations and to N.A. Beisen for the hospitality and provision of the observational time at the “Bobek” observatory.

## References

- Bruch, A. and Schimpke, T.: 1992, *Astron. Astrophys., Suppl. Ser.* **93**, 419
- Bruch, A., Fischer, F.-J. and Wilmsen, U.: 1987, *Astron. Astrophys., Suppl. Ser.* **70**, 481
- Fridman, A.M., Boyarchuk, A.A., Bisikalo, D.V., Kuznetsov, O.A., Khoruzhii, O.V., Torgashin, Y.M., and Kilpio, A.A.: 2003, *Physics Letters A* **317**, 181
- Fridman, A.M. and Bisikalo, D.V.: 2008, *Physics Uspekhi* **51**, 551
- Fridman, A.M. and Khoruzhii, O.V.: 2003, *Space Sci. Rev.* **105**, 1
- Gessner, H.: 1966, *Veroeffentlichungen der Sternwarte Sonneberg* **7**, 61
- Harvey, D., Skillman, D.R., Patterson, J., and Ringwald, F.A.: 1995, *Publ. Astron. Soc. Pac.* **107**, 551
- Hellier, C.: 2001, *Book: Cataclysmic Variable Stars, Springer*, , 1
- Henden, A. and Munari, U.: 2006, *Astron. Astrophys.* **458**, 339
- Hirose, M. and Osaki, Y.: 1990, *PAS of Japan* **42**, 135
- Hoffmeister, C.: 1963a, *Astron. Nachr.* **287**, 169
- Hoffmeister, C.: 1963b, *Zentralinstitut fuer Astrophysik, Sternwarte Sonneberg - Mitteilungen ueber Veraenderliche Sterne*, , No 751
- Hoshi, R.: 1979, *Progress of Theoretical Physics* **61**, 1307
- Kato, T., Imada, A., Uemura, M., Nogami, D., Maehara, H., Ishioka, R., Baba, H., Matsumoto, K., Iwamatsu, H., et al.: 2009, *PAS of Japan* **61**, 395
- Kato, T., Nogami, D., Baba, H., Masuda, S., Matsumoto, K., and Kunjaya, C.: 2013, *ArXiv e-prints* **1301**, 3202
- Kato, T.: 2015, *PAS of Japan* **67**, 108
- Kato, T., Pavlenko, E.P., Shchurova, A.V., Sosnovskij, A.A., Babina, J.V., Baklanov, A.V., Shugarov, S.Y., Littlefield, C., Dubovsky, P.A., Kudzej, I., Pickard, R.D., Isogai, K., Kimura, M., de Miguel, E., Tordai, T., Chochol, D., Maeda, Y., Cook, L.M., Miller, I., and Itoh, H.: 2016, *PAS of Japan* **68**, L4
- Kato, T., Isogai, K., Hamsch, F.-J., Vanmunster, T., Itoh, H., Monard, B., Tordai, T., Kimura, M., Wakamatsu, Y., Kiyota, S., Miller, I., Starr, P., Kasai, K., Shugarov, S.Y., Chochol, D., Katysheva, N., Zaostrojnnykh, A.M., Sekeráš, M., Kuznyetsova, Y.G., Kalinicheva, E.S., Golyшева, P., Krushevska, V., Maeda, Y., Dubovsky, P.A., Kudzej, I., Pavlenko, E.P., Antonyuk, K.A., Pit, N.V., Sosnovskij, A.A., Antonyuk, O.I., Baklanov, A.V., Pickard, R.D., Kojiguchi, N., Sugiura, Y., Tei, S., Yamamura,

- K., Matsumoto, K., Ruiz, J., Stone, G., Cook, L.M., de Miguel, E., Akazawa, H., Goff, W.N., Morelle, E., Kafka, S., Littlefield, C., Bolt, G., Dubois, F., Brincat, S.M., Maehara, H., Sakanoi, T., Kagitani, M., Imada, A., Voloshina, I.B., Andreev, M.V., Sabo, R., Richmond, M., Rodda, T., Nelson, P., Nazarov, S., Mishevskiy, N., Myers, G., Denisenko, D., Stanek, K.Z., Shields, J.V., Kochanek, C.S., Holoiien, T.W.-S., Shappee, B., Prieto, J.L., Itagaki, K.-i., Nishiyama, K., Kabashima, F., Stubbings, R., Schmeer, P., Muylaert, E., Horie, T., Shears, J., Poyner, G., and Moriyama, M.: 2017a, *PAS of Japan* **69**, 75
- Kato, T., Tordai, T., Littlefield, C., Kasai, K., Shugarov, S.Y., Katysheva, N., Zaostrojnkh, A.M., Pickard, R.D., de Miguel, E., Antonyuk, K., Antonyuk, O., Pavlenko, E.P., Pit, N., Itoh, H., Ruiz, J., Isogai, K., Kimura, M., Wakamatsu, Y., Vanmunster, T., and Stone, G.: 2017b, *PAS of Japan* **69**, L4
- Knigge, C.: 2006, *Mon. Not. R. Astron. Soc.* **373**, 484
- Lubow, S.H.: 1991, *Astrophys. J.* **381**, 259
- Meyer, F. and Meyer-Hofmeister, E.: 1981, *Astron. Astrophys.* **104**, L10
- Osaki, Y.: 1989, *PAS of Japan* **41**, 1005
- Osaki, Y.: 1996, *Publ. Astron. Soc. Pac.* **108**, 39
- Pavlenko, E.P., Shugarov, S.Y., Baklanova, D.N., and Katysheva, N.A.: 2008, *Izv. Krymskoj Astrofiz. Obs.* **104**, 109
- Pavlenko, E.P., Kato, T., Sosnovskij, A.A., Andreev, M.V., Ohshima, T., Sklyanov, A.S., Bikmaev, I.F., and Galeev, A.I.: 2014, *PAS of Japan* **66**, 113
- Pavlenko, E.P. and Shugarov, S.Y.: 1999, *Astron. Astrophys.* **343**, 909
- Pavlenko, E.P.: 1996, *Odessa Astronomical Publications* **9**, 38
- Pelt, Y.: 1980, *Book: Frequency analysis of astronomical time series*, Tallin, Valgus, 135
- Ringwald, F.A., Velasco, K., Roveto, J.J., and Meyers, M.E.: 2012, *New Astronomy* **17**, 433
- Scaringi, S.: 2017, *Nature* **552**, 210
- Sheets, H.A., Thorstensen, J.R., Peters, C.J., Kapusta, A.B., and Taylor, C.J.: 2007, *Publ. Astron. Soc. Pac.* **119**, 494
- Sklyanov, A.S., Pavlenko, E.P., Antonyuk, O.I., Sosnovskij, A.A., Malanushenko, V.P., Pit, N.V., Antonyuk, K.A., Khairutdinova, A.N., Babina, Yu.V., and Galeev, A.I.: 2018, *Astrofizika* **61**, 79
- Shugarov, S., Katysheva, N., Chochol, D., Gladilina, N., Kalinicheva, E., and Dodin, A.: 2016, *Contrib. Astron. Obs. Skalnaté Pleso* **46**, 5
- Smak, J.: 1987, *Astrophys. Space Sci.* **131**, 497
- Udalski, A.: 1988, *Acta Astron.* **38**, 315
- Warner, B.: 1995, *Cambridge Astrophysics Series* **28**, 1
- Whitehurst, R.: 1988, *Mon. Not. R. Astron. Soc.* **232**, 35
- Wood, M.A., Still, M.D., Howell, S.B., Cannizzo, J.K., and Smale, A.P.: 2011, *Astrophys. J.* **741**, 105
- Wood, M.A. and Burke, C.J.: 2007, *Astrophys. J.* **661**, 1042
- Wood, M.A., Thomas, D.M., and Simpson, J.C.: 2009, *Mon. Not. R. Astron. Soc.* **398**, 2110
- Zemko, P., Shugarov, S., Kato, T., and Katysheva, N.: 2014, *Contrib. Astron. Obs. Skalnaté Pleso* **43**, 319